JOURNAL OF BACTERIOLOGY, Apr. 1997, p. 2259–2266 Vol. 179, No. 7
0021-9193/97/$04.00+0

In Vivo Nickel Insertion into the Carbon Monoxide Dehydrogenase of *Rhodospirillum rubrum*: Molecular and Physiological Characterization of *cooCTJ*

R. L. KERBY,[1,2] P. W. LUDDEN,[2] AND G. P. ROBERTS[1]*

Departments of Bacteriology[1] and Biochemistry,[2] College of Agricultural and Life Sciences, University of Wisconsin-Madison, Madison, Wisconsin 53706

Received 21 August 1996/Accepted 24 January 1997

The products of *cooCTJ* are involved in normal in vivo Ni insertion into the carbon monoxide dehydrogenase (CODH) of *Rhodospirillum rubrum*. Located on a 1.5-kb DNA segment immediately downstream of the CODH structural gene (*cooS*), two of the genes encode proteins that bear motifs reminiscent of other (urease and hydrogenase) Ni-insertion systems: a nucleoside triphosphate-binding motif near the N terminus of CooC and a run of 15 histidine residues regularly spaced over the last 30 amino acids of the C terminus of CooJ. A $Gm^r\Omega$-linker cassette was developed to create both polar and nonpolar (60 bp) insertions in the *cooCTJ* region, and these, along with several deletions, were introduced into *R. rubrum* by homologous recombination. Analysis of the exogenous Ni levels required to sustain CO-dependent growth of the *R. rubrum* mutants demonstrated different phenotypes: whereas the wild-type strain and a mutant bearing a partial *cooJ* deletion (of the region encoding the histidine-rich segment) grew at 0.5 μM Ni supplementation, strains bearing $Gm^r\Omega$-linker cassettes in *cooT* and *cooJ* required approximately 50-fold-higher Ni levels and all *cooC* insertion strains, bearing polar or nonpolar insertions, grew optimally at 550 μM Ni.

The phototrophic bacterium *Rhodospirillum rubrum* induces synthesis of an Ni- and Fe-containing carbon monoxide dehydrogenase (CODH) upon anaerobic exposure to CO (3, 4) and couples CO oxidation to H_2 evolution as a source of energy (31). Limited evidence suggests that accessory functions are necessary for posttranslational Ni insertion and CODH activity in *R. rubrum*: an Ni-deficient apo-CODH is found in induced cultures deprived of Ni; substantially higher Ni concentrations are required for activation of apo-CODH in vitro than in vivo; and there is an elevated Ni requirement for CO-dependent growth of a mutant bearing an insertion in *cooC*, a gene immediately downstream of the CODH structural gene (5, 13, 31).

Aside from the physiology of Ni insertion, the *R. rubrum* CODH has been well characterized biochemically (4, 14), genes encoding its synthesis and several additional proteins likely involved in H_2 production have been cloned and sequenced (16, 17, 30), active CODH has been heterologously expressed (24), and the CO-responsive transcriptional regulator is under investigation (24, 53). The hydrogenase (CooH) and CODH (CooS) genes occur in two operons, *cooMKLXUH* and *cooFSCTJ*, whose coding regions are separated by a 450-bp interval, with the CO-responsive transcriptional activator (CooA) encoded 137 nucleotides downstream of *cooJ*.

Formation of the Ni-containing center(s) of other Ni-CODH enzymes has not been characterized, although the activities are prevalent in diverse anaerobic archaea and bacteria (15). Both the spectroscopic similarities of purified enzymes (26) and evident conservation of a limited number of potential metal ligands in an alignment of bacterial and archaeal CODH sequences (e.g., see reference 30) are consistent with conservation of structure and function of the Ni-containing C center, the site of CO oxidation, and could imply similarities in C-center synthesis.

Metal center formation in the three classes of Ni-containing enzymes apart from Ni-CODH has been characterized to various degrees. Synthesis and insertion of the porphinoid Ni cofactor of methyl coenzyme M reductase is relatively undefined (57), while molecular analyses of hydrogenase- and urease-associated systems are better elaborated. For example, synthesis of active hydrogenase 3 in *Escherichia coli* depends on an Ni-transport system (encoded by *nikABCDE*), elements required for Ni insertion (encoded by *hypABCDEF*), and C-terminal proteolytic processing of the hydrogenase large subunit (HycE) by a specific protease (HycI). Ni transport (e.g., NixA and UreH), Ni processing (encoded by *ureEFG*), and chaperonin-like (UreD) functions are affiliated with various ureases. Recent reviews summarize the urease and hydrogenase Ni-insertion systems (39, 43, 44) and note the presence of nucleotide-binding and histidine-rich motifs in each.

Here, we characterize the 1.5-kb DNA segment bearing *cooCTJ*, compare the functions of the three encoded proteins to hydrogenase and urease accessory functions, and describe the CO- and Ni-dependent growth characteristics of mutant *R. rubrum* strains bearing polar and nonpolar insertions in this region. A modified $Gm^r\Omega$ cassette was used to generate the insertion mutants.

MATERIALS AND METHODS

Cultivation and DNA isolation. Formulations of media (for non-CO-dependent growth), bacterial growth conditions, and plasmid and chromosomal DNA isolations have been described (30). Antibiotics used (micrograms per milliliter) included gentamicin sulfate, 7.5 (*E. coli*) or 10 (*R. rubrum*); kanamycin sulfate, 50 (*E. coli*) or 15 (*R. rubrum*); ampicillin (Na salt), 100 (*E. coli*); streptomycin sulfate, 20 (*E. coli*) or 100 (*R. rubrum*); and nalidixic acid (Na salt), 20 (*R. rubrum*). *R. rubrum* recipients of triparental matings were selected by inclusion of 10 μg of K_2TeO_3 per ml.

CO-dependent growth analyses. CO-dependent growth used SAN medium wherein the malate in SMN medium (30, 31) was replaced by 0.82 g of Na acetate per liter as a nonfermentable carbon source. The inclusion of 0.3% Casamino enzymatic hydrolysate (catalog no. C-0626; Sigma, St. Louis, Mo.) was crucial in

* Corresponding author. Mailing address: Department of Bacteriology, 1550 Linden Dr., Madison, WI 53706. Phone: (608) 262-3567. Fax: (608) 262-9865. E-mail: groberts@bact.wisc.edu.

preventing Ni toxicity at high Ni concentrations and primarily reflected its histidine and cysteine content. Growth on plates was performed by a method previously described (31) except that the plates were incubated in 19-1 glass carboys prepared as follows: after an overnight reduction phase, achieved through a combination of evacuation, flushing with Ar, and H_2/CO_2 generation by three GasPak envelopes in the presence of 20 g of palladium catalyst (BBL Microbiology Systems, Cockeysville, Md.) per vessel, oxygen-free CO was added to ca. 20% at an initial pressure of 2 lb/in^2 above atmospheric pressure. For CO-dependent growth, vessels were incubated in the dark at 30°C; the pressure was adjusted when required as each mole of CO consumed produces nearly 2 mol of gaseous products (CO_2 and H_2) (31). Ni supplements were prepared with $NiCl_2 \cdot 6H_2O$ (catalog no. 6376 Mallinckrodt, Paris, Ky.). Cobalt supplements were prepared with $CoCl_2 \cdot (5–6)H_2O$, 99.999% (cat. no. 20,308-4; Aldrich, Milwaukee, Wis.). High-purity CO (99.99%, rendered O_2-free [13]; Liquid Carbonic Specialty Gas Co., Chicago, Ill.) was used.

Gm^{r}Ω-linker cassette synthesis and structure. We modified a Gm^{r}Ω cassette (52) by inserting it into a 60-bp linker, creating an *aacC1Ωlinker* construct. After insertion of the construct into the *coo* region, *Bam*HI-catalyzed excision of the Gm^{r}Ω cassette and subsequent religation left the 60-bp linker fragment inserted. The palindromic linker consists of a blunt-ended (*Sma*I) DNA fragment with the following sequence (one strand shown, central *Bam*HI site in bold): 5′-GGGT TTCCCCGTTTCCGCTGCAGCTGC**GGATCC**GCAGCTGCAGCGGAAAC GGGGAAACCC-3′. The linker is readily translated in all reading frames, with a codon usage approximating that of *R. rubrum*, resulting in one of three 20-amino-acid insertions in the final gene product. Strains with the nonpolar linker insertion genotype are designated by the suffix "*linker*" in Table 1 and below.

Construction of the linker started with a high-performance liquid chromatography-purified 35-base oligonucleotide (Operon Technologies, Inc., Alameda, Calif.), self-complementary for 10 bases at the 3′ end, that was hybridized and extended (46) using Sequenase version 2.0 DNA polymerase (United States Biochemical, Cleveland, Ohio). The resulting fragment was purified from a native 10% acrylamide gel and cloned into the *Sma*I site of pBSKS−, yielding pCO18. The structure of the linker was verified by sequencing, and the *Bam*HI-excised Gm^{r}Ω cassette from pGMΩ1 (52) was then cloned into the linker *Bam*HI site to yield the *aacC1Ωlinker*-bearing pCO19.

Plasmid construction and generation of *R. rubrum* mutants. Table 1 indicates the relevant plasmid constructs, organized according to their general or mutation-specific application, used in creating *cooCTJ*-region mutants. In general, plasmids bearing cassette insertions were derived from several *coo*-region subclones using complete or partial digests (single cut in the presence of ethidium bromide [47]) of target DNA, blunting of ends (for the *cooJ* insertions) with Klenow polymerase (Promega, Madison, Wis.), and ligation with the *Sma*I-excised *aacC1Ωlinker* cassette by standard methods (51; Table 1). Nonmobilizable constructs were moved to mobilizable pUX19 derivatives bearing flanking *coo*-region DNA sufficient for subsequent recombination into the *R. rubrum* chromosome. All pUX19 derivatives lacked the multiple cloning region *Bam*HI site, permitting generation of nonpolar linker insertions as well as *aacC1Ωlinker* insertions of reversed orientation by *Bam*HI digestion, religation, transformation, and selection or screening for Km^{r}Gm^r (*aacC1Ωlinker* insertion) or Km^r Gm^s (*linker* insertion) transformants. Gm^r constructs were moved to *E. coli* UQ324(S17-1) (54), verified, and used in filter-supported mating to *R. rubrum* UR2 (36) with selection for Nx^r and Gm^r and screening for Km^s, thereby indicating reciprocal homologous recombination of the mutated DNA into the chromosome. The nonpolar *cooT19*::*linker* and Δ*cooJ18* constructs were mated to *R. rubrum* UR452, while the nonpolar *cooC20*::*linker* and *cooC21*::*linker* derivatives were mated to *R. rubrum* UR469 and UR447, respectively, in triparental matings with *E. coli* UQ377 (22). Isolated Te^{r}Km^r merodiploids were resolved by a period of nonselective outgrowth in SMN medium supplemented with nalidixic acid, plating on SMN-nalidixic acid plates, and screening for both Km^s and Gm^s.

Mutations were verified by restriction analyses of the plasmid constructs, with retention of the *Sma*I junction of the *cooC* and *cooT* insertions of particular note, sequencing (Δ*cooJ18*), and Southern analysis of isolated mutant *R. rubrum* chromosomal DNA (all strains, data not shown).

Sequence analyses. DNA sequencing depended on preparation of nested exonuclease III deletions (as modified [30]) of pCO4 (*cooC* region) and pCO5 (*cooCTJ* and 5′-*cooA*) in one direction, with sequencing reactions primed using commercial primers, and use of custom primers (Department of Biochemistry oligonucleotide facility, Univ. of Wisconsin-Madison) to sequence the complementary strand. As previously detailed (53), highly denaturing urea-formamide gels and use of deaza-dGTP or dITP nucleotides as well as terminal transferase modifications of the Sequenase version 2.0 reaction (United States Biochemical) were employed to resolve compression artifacts and eliminate pausing. Complementary DNA strands were sequenced in their entirety and analyzed using the Genetics Computer Group version 8 (Wisconsin package) software (19). Protein database searches employed the BLAST network server (2); hydropathy predictions relied on the protein sequence analysis server (56, 60).

2D PAGE analyses. Log-phase cultures growing photosynthetically in MN medium (30) supplemented with 50 μM Ni were induced by introduction of CO to 10% (vol/vol headspace; control, Ar) for 30 min, after which 1-ml samples were transferred to illuminated anaerobic vials containing the same headspace plus 75 μCi of Tran^{35}S-label (ca. 70% Met–15% Cys; ICN Pharmaceuticals, Inc., Irvine, Calif.). After 10 min of further incubation, 0.6-ml samples were transferred to precooled 1.5-ml microcentrifuge tubes and stored frozen (−80°C) until processed and analyzed by two-dimensional polyacrylamide gel electrophoresis (2D-PAGE) (3).

Nucleotide sequence accession number. The region characterized in this article appears in the GenBank sequence database under accession no. U65510, in a compilation that includes flanking *coo* DNA.

RESULTS

Encoded proteins. The sequence of the 1.5-kb region between *cooS* and *cooA* indicated three open reading frames with codon usage and G + C content (64%) appropriate for *R. rubrum* (Fig. 1). The genes overlap, suggesting translational coupling, and are apparently transcribed as part of the *coo FSCTJ* mRNA upon CO activation of CooA (24, 53). The *cooC* gene is predicted to start 67 nucleotides downstream from *cooS* and encodes a predicted product of 263 amino acids (27.8 kDa, pI = 6.09) (Fig. 2). Hydropathy algorithms indicated little probability of transmembrane segments (56, 60). As noted previously (30), CooC (formerly ORF4) contains a nucleotide-binding P-loop motif near the N terminus (Fig. 2), and this region aligns well with NifH proteins as well as with regions of the accessory proteins that support Ni insertion in urease (e.g., UreG [44]) and hydrogenase (e.g., HypB [39]) systems. Similarities among these proteins beyond the CooC N terminus are less compelling, although the CooC Gly-Arg-Gly segment (centered in residues 140 to 162) is notable considering the role of the similar sequence in NifH interaction with dinitrogenase component I and in posttranslational regulation (37, 48). NifH is also required for MgATP-dependent FeMo-co insertion into apo-dinitrogenase (1).

Recent analyses show significant similarities over the length of CooC to the ORF1 predicted protein of *Methanosarcina thermophila* (57% similarity [41]), which occurs within this organism's *cdh* operon, as well as to the MJ0823 predicted protein of *Methanococcus jannaschii* (63% similarity [7]).

The ATG of the downstream *cooT* gene overlaps *cooC* by one base and is predicted to encode a 7.1-kDa acidic protein of 66 amino acids (pI = 4.81; Fig. 2) that is moderately hydrophobic (56, 60). The single cysteine in CooT excludes it as a common Fe/S center (ferredoxin) or metal-chelating (metallothionen) protein, which typically contain multiple cysteines. Protein database searches indicated marginal overall similarities with other entries, including the small, acidic, low-Cys-content HypC protein family (39); several of the latter proteins bear an N-terminal sequence identical to CooT: Met-Cys-xxx-Ala. The *Alcaligenes eutrophus* HypC is essential for hydrogenase formation, although its precise role is undefined (11).

The third ORF, *cooJ*, overlaps *cooT* by four nucleotides and encodes a 12.6-kDa, intrinsically soluble (56, 60) 115-amino-acid protein with a predicted pI of 6.46 (Fig. 2). The N-terminal 11 amino acids, starting at the second-position threonine, have been verified by sequencing the purified protein (58). Of the C-terminal 30 amino acids, 15 histidines alternate with another amino acid (typically S, D, or C), and CooJ is thereby similar to several histidine-rich UreE and HypB accessory proteins thought to participate in Ni processing in urease and hydrogenase systems, respectively (39, 44).

Generation of polar and nonpolar mutants by linker insertion and verification of appropriate polarity. By inserting a Gm^r (*aacC1*) Ω cassette into a 60-bp blunt-ended DNA segment, we created a polar cassette (*aacC1Ωlinker*) from which a nonpolar insertion (*linker*) could be derived upon excision of the resistance marker, assuming that the target insertion site was also blunt ended. Unlike protocols that create shorter (equivalent to two to four amino acid) insertions for localized

TABLE 1. Relevant characteristics of strains and plasmids

Plasmid and/or strain[a]	Characteristics[b] or derivation	Reference or source[c]
Plasmids/*E. coli* strains used in construction of various mutations		
pBSKS−/UQ625	Ap^r *lacZ′*, in *E. coli* DK1	Stratagene[d]
pCO4/UQ1191	Ap^r, 3.3-kb *Eco*RV fragment bearing *coo′HFSC′*, subcloned from pLJC24 into pBSKS−	
pCO5/UQ1193	Ap^r, 1.5-kb *Eco*RV fragment bearing *coo′CTJA′*, subcloned from pLJC24 into pBSKS−	
pCO6/UQ1045	Km^r *mob*$^+$, 8.5-kb *Eco*RI fragment transferred from pLJC24 into pUX19	
pCO6R/UQ1046	Same as pCO6, opposite insert orientation	
pCO15/UQ1164	Km^r *mob*$^+$, pCO6 with vector *Bam*HI site deleted	
pCO18/UQ1231	Ap^r, pBSKS− with the 60-bp linker inserted at the *Sma*I site	
pCO19/UQ1232	Ap^r Gm^r, pCO18 with the *Bam*HI-excised Gm^{r}Ω cassette from pGMΩ1 inserted into the linker *Bam*HI site	
pCO24R/UQ1241	Km^r *mob*$^+$, pCO6R with 2.5-kb *Bgl*II fragment deleted; insert bears *cooUHFSCTJ*	
pCO25R/UQ1243	Km^r *mob*$^+$, pCO24R with vector *Bam*HI site deleted	
pCO33/UQ1246	Ap^r, 4.5-kb *Apa*I fragment bearing *coo′SCTJA* + *nad′C* from pLJC24 subcloned into pBSKS− (*Apa*I site internal to *cooJ* Dcm methylated)	
pCO34/UQ1273	Ap^r, pCO33 with vector *Eco*RI-*Bam*HI region deleted	
pGMΩ1/UQ1152	Gm^r (*aacC1*) within an Ω cassette, in UQ500	52
pLJC24/UQ1242	Ap^r, 8.5-kb *Eco*RI fragment bearing *cooUHFSCTJA* and *nad′BC*, cloned into pUC118	9
pUX19/UQ837	Km^r *mob*$^+$, does not replicate in *R. rubrum*	36
Plasmids/*E. coli* strains used for construction of Δ(*cooS′CTJ*)*14*::*aac1*Ω◂		
pCO39/UQ1289	Ap^r, Δ(*Xho*I-*Bam*HI) in pCO33 vector MCS	
pCO40/UQ1290	Ap^r Gm^r, pCO39 Δ(*Hin*dIII-*Bgl*II), Klenow blunted, ligated to *aacC1*Ω/*Sma*I cassette from pGMΩ1	
pCO58/UQ1306	Km^r Gm^r *mob*$^+$, *Pvu*II fragment from pCO40 inserted into pUX19	
Plasmids/*E. coli* strains used for construction of Δ(*cooFSCTJA*)*10*::*aacC1*Ω◂		
pCO26R2/UQ1245	Km^r Gm^r *mob*$^+$, pCO6R/*Xcm*I vector portion, Klenow blunted and ligated to *aacC1*Ω/*Sma*I cassette from pGMΩ1	
Plasmids/*E. coli* strains used for construction of *cooJ22* and *cooJ23* insertions		
pCO59/np[e]	Ap^r Gm^r, pCO5/*Nar*I (Klenow blunted) ligated to *aacC1*Ω*linker*▸/*Sma*I cassette from pCO19	
pCO60/np[e]	Ap^r Gm^r, pCO5/*Nar*I (Klenow blunted) ligated to *aacC1*Ω*linker*◂/*Sma*I cassette from pCO19	
pCO61/UQ1349	Km^r Gm^r *mob*$^+$, pCO15 with *Hpa*I-*Xmn*I fragment replaced with mutated segment from pCO59	
pCO62/UQ1348	Km^r Gm^r *mob*$^+$, pCO15 with *Hpa*I-*Xmn*I fragment replaced with mutated segment from pCO60	
Plasmids/*E. coli* strains used for construction of the *cooC12*, *cooC16*, and *cooC20* insertions (at the *Sma*I site)		
pCO31R/UQ1271	Km^r Gm^r *mob*$^+$, pCO25R/*Sma*I (partial) ligated with *aacC1*Ω*linker*▸/*Sma*I cassette from pCO19	
pCO49R/UQ1327	Km^r Gm^r *mob*$^+$, *cooC*::*aacC1*Ω*linker*◂ derived from pCO31R	
pCO50R/UQ1328	Km^r *mob*$^+$, *cooC*::*linker* insertion derived from pCO31R	
Plasmids/*E. coli* strains used for construction of the *cooC11*, *cooC15*, and *cooC21* insertions (at the *Hpa*I site)		
pCO28R/UQ1268	Km^r Gm^r *mob*$^+$, pCO25R/*Hpa*I ligated with *aacC1*Ω*linker*◂/*Sma*I cassette from pCO19	
pCO51R/UQ1329	Km^r Gm^r *mob*$^+$, *cooC*::*aacC1*Ω*linker*▸ derived from pCO28R	
pCO52R/UQ1330	Km^r *mob*$^+$, *cooC*::*linker* insertion derived from pCO28R	
Plasmids/*E. coli* strains used for construction of the *cooT13*, *cooT17*, and *cooT19* insertions		
pCO35-1/UQ1274	Ap^r Gm^r, pCO5/*Sma*I (partial) ligated with *aacC1*Ω*linker*▸/*Sma*I cassette from pCO19	
pCO41/UQ1291	Km^r Gm^r *mob*$^+$, pCO15 with *Hpa*I-*Xmn*I fragment replaced with mutated segment from pCO35-1	

Continued on following page

TABLE 1—*Continued*

Plasmid and/or strain[a]	Characteristics[b] or derivation	Reference or source[c]
pCO53/UQ1331	Km^r Gm^r *mob*$^+$, *cooT*::*aacC1*Ω*linker*◂ derived from pCO41	
pCO54/UQ1332	Km^r *mob*$^+$, *cooT*::*linker* insertion derived from pCO41	
Plasmids/*E. coli* strains used in construction of Δ*cooJ18*		
pCO29/UQ1267	Ap^r, pCO5 (isolated from UQ580 host) with 60-bp *Bcl*I-*Bcl*I fragment of *cooJ* deleted	
pCO38/UQ1288	Ap^r, *Pst*I-*Bgl*II fragment of pCO34 replaced by region from pCO29 bearing the *cooJ* deletion	
pCO48/UQ1309	Km^r *mob*$^+$, 4.5-kb insert region from pCO38 moved as a *Kpn*I-*Xho*I fragment into pUX19	
E. coli strains		
UQ324(S17-1)	Nx^s Sm^r *recA*, RP4 *tra* functions	54
UQ377(MM294A)	Te^s Km^r *endA1* [pRK2013 with RK2 *tra* functions]	G. Walker[f]
UQ500(DH5α)	Nx^r *recA1 endA1 lacZ*ΔM15	BRL[g]
UQ555(XL1-Blue)	Nx^r Tc^r *recA1 endA1 lac* [F′::Tn*10 proAB lacI*^{q}*Z*ΔM15]	Stratagene
UQ580	*dam*	C. Gross[h]
R. rubrum strains		
UR2	Nx^r, spontaneous Sm^r derivative of wild-type strain S1	P. W. Ludden
UR294	UR2 Sm^r Nx^r Km^r *cooC7*::*kan*	25
UR445	UR2 Sm^r Nx^r Gm^r Δ(*cooFSCTJA*)*10*::*aacC1*Ω◂	
UR447	UR2 Sm^r Nx^r Gm^r *cooC11*::*aacC1*Ω*linker*◂	
UR449	UR2 Sm^r Nx^r Gm^r *cooC12*::*aacC1*Ω*linker*▸	
UR451	UR2 Sm^r Nx^r Gm^r *cooT13*::*aacC1*Ω*linker*▸	
UR452	UR2 Sm^r Nx^r Gm^r Δ(*cooS′CTJ*)*14*::*aacC1*Ω◂	
UR468	UR2 Sm^r Nx^r Gm^r *cooC15*::*aacC1*Ω*linker*▸	
UR469	UR2 Sm^r Nx^r Gm^r *cooC16*::*aacC1*Ω*linker*◂	
UR470	UR2 Sm^r Nx^r Gm^r *cooT17*::*aacC1*Ω*linker*◂	
UR471	UR2 Sm^r Nx^r Δ*cooJ18*	
UR479	UR2 Sm^r Nx^r *cooT19*::*linker*	
UR495	UR2 Sm^r Nx^r *cooC20*::*linker*	
UR497	UR2 Sm^r Nx^r *cooC21*::*linker*	
UR500	UR2 Sm^r Nx^r Gm^r *cooJ22*::*aacC1*Ω*linker*▸	
UR501	UR2 Sm^r Nx^r Gm^r *cooJ23*::*aacC1*Ω*linker*◂	

[a] Host strain for pCOxx constructs is *E. coli* UQ555, unless noted.
[b] Transcriptional orientation of the *aacC1* (Gm^r) gene within the Ω cassette is denoted by ▸ or ◂ relative to left to right transcriptional orientation of *cooFSCTJ*. The *aacC1*Ω*linker* and *linker* designations indicate the polar Gm^r linker cassette and nonpolar 60-bp linker insertion, respectively.
[c] If not this study.
[d] Stratagene Cloning Systems, La Jolla, Calif.
[e] Not preserved.
[f] Graham Walker, Massachusetts Institute of Technology, Cambridge.
[g] BRL, Bethesda Research Laboratories, Gaithersburg, Md.
[h] Carol Gross, University of California, San Francisco.

linker scanning mutagenesis (and may yield functional proteins [21, 28]) or that create longer reading-frame-specific insertions for epitope tagging purposes (32), the goal here modified the original "interposon" idea (49) to create a larger insertion that, when translated in any reading frame, should be sufficiently disruptive to eliminate the function of the targeted gene product without affecting synthesis of those encoded downstream. The nonpolar mutations were then recombined into the *R. rubrum* chromosome, using recipients either deleted for the mutated region (UR452) or already bearing an *aacC1*Ω*linker* at the appropriate site (UR469 or UR447) in screening for desired recombination events.

To test for polarity, as well as to examine effects on the mutated gene product, strains were pulse-labelled with [^{35}S]Met/Cys and analyzed by 2D-PAGE and autoradiography. We were unable to identify a protein spot as CooT, possibly reflecting its small size and low number of Met and Cys residues (three total, assuming retention of the N-terminal Met). CO-induced *cooC* and *cooJ* products were evident, although the latter migrated at an unexpectedly high molecular mass (ca. 19 kDa), consistent with results observed with the purified protein (58) and other histidine-rich proteins (18, 20, 50). Synthesis of CooC in strains with insertions downstream of *cooC*, e.g., UR479 (Fig. 3, upper panel), approximated that in wild-type strain UR2 (Fig. 3), while CooJ was detected only in wild-type and nonpolar *cooC* or *cooT* insertion strains (UR2, UR479, and UR495; Fig. 3, lower panel). 2D-PAGE analysis of extracts from UR471 (Δ*cooJ18*) also lacked a protein spot at the position of CooJ but exhibited a smaller protein of appropriate charge for the deletion product (data not shown). Proteins derived from the linker-modified *cooC* of UR495 and UR497 were not detected, indicating either that the modified proteins (in each case bearing a different 20-amino-acid insert but of similar predicted pI [6.50] and size [ca. 30 kDa]) were very rapidly degraded or obscured by other proteins. Thus, the Gm^r cassette insertions were polar onto cotranscribed downstream genes (specifically, *cooJ*), while the nonpolar insertions, insofar as we are able to assess the synthesis of CooC and CooJ, affected only the targeted gene product.

General physiology of *cooC*, *-T*, and *-J* mutants. The mutant strains grew normally under aerobic conditions in SMN medium; photoautotrophic growth of UR469 (*cooC16*::*aacC1*Ω*linker*) and UR2 were identical and were comparably enhanced by low levels (10 μM) of Ni in the medium (data not shown). This Ni

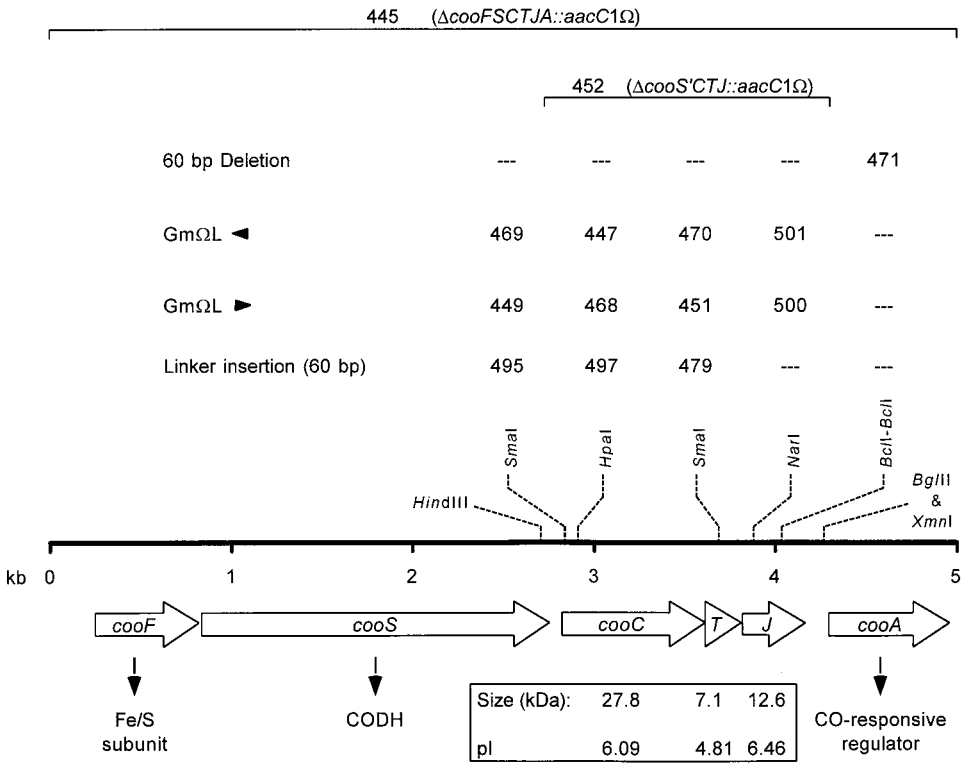

FIG. 1. Organization of *cooFSCTJA*. Arrows below the scale indicate gene designations and relevant properties of the predicted proteins. Above the scale are the *R. rubrum* UR strain numbers that designate mutants bearing nonpolar 60-bp *linker* ("Linker") insertions, polar *aacC1Ωlinker* cassette ("GmΩL") insertions (*aacC1* transcriptional orientation denoted by a ► or ◄ suffix), and *coo*-region deletions. The mutation position is indicated by the placement of the UR number over a specific restriction site; the extent of the UR445 and UR452 deletion/insertion constructs is designated by horizontal brackets. UR471 contains a 60-bp deletion between two *Bcl*I sites in *cooJ*. Not shown are the *cooMKLXUH* transcript, which extends 8 kb 5′ of *cooF* (16, 17) and is likewise transcribed from left to right, and the *nad′BC* region, which lies 3′ of *cooA* (53).

enhancement is consistent with the involvement of an Ni hydrogenase in H_2 uptake during photoautotrophic growth and suggests that global Ni transport/metabolism functions have not been altered.

Ni requirement of CO-dependent growth. To examine effects of Ni concentration in the medium on CO-dependent growth, we employed plate growth assays using rich (SAN) medium because (i) the method allowed determination of growth of dense (patch plate) and dilute (streak plate) inocula; (ii) the Na_2S addition routinely used for CO-dependent growth in liquid culture (31) was unnecessary, thus avoiding Ni precipitation as NiS; (iii) effects of subtle variations in the medium were avoided by comparing several strains on the same plate; and (iv) the chelation of Ni by the casein enzymatic hydrolysate (particularly the cysteine and histidine components) prevented significant Ni toxicity at Ni levels as high as 650 μM (Casamino Acids could be replaced by 100 to 300 μM EDTA). Even in this rich medium, growth of *R. rubrum* anaerobically in the dark was dependent on Ni supplementation and CO oxidation as a source of energy. Note that the medium contains acetate as a carbon source.

When approximately 10^4 cells in 2 μl were spotted onto SAN plates and incubated anaerobically with CO, all strains grew photosynthetically without addition of Ni (Fig. 4). In contrast, CO-dependent growth of strain UR2 (wild type) in the dark required Ni supplementation, and a mutant strain (UR445) lacking *cooFSCTJA* failed to grow on CO regardless of the medium Ni level. The *cooC*, *-T*, and *-J* mutant strains exhibited three basic Ni-dependent CO growth phenotypes: (i) UR471 and UR479 resembled the wild-type strain and grew at a low (0.5 μM) Ni concentration; (ii) UR470 and UR501 required an approximately 50-fold-higher Ni concentration than did the wild type, with growth enhanced by further increases in [Ni]; and (iii) *cooC* strains required an approximately 1,000-fold-higher Ni concentration than the wild type. These phenotypes were independent of insert orientation (data not shown), placement (in *cooC*, data not shown), and, in the case of the *cooC* mutations, polarity (compare UR469 and UR495, Fig. 4).

Subtle but reproducible variations in CO-dependent growth were noted within these basic groupings, in particular the unanticipated ability of UR479 to grow better than UR2 on non-Ni-supplemented medium (Fig. 4) and in liquid culture (data not shown), yet not as well as UR2 at Ni levels between 2 and 225 μM (as determined by colony size on streaked plates; data not shown). The slight growth of UR471 in the absence of Ni additions (Fig. 4) was never as obvious as the UR479 phenotype. The *cooC* mutant strains also exhibited a subtle variation: 550 μM Ni supported optimal growth of all strains, but strains bearing the nonpolar insertions (UR495 and 497) grew better than the polar insertion strains (UR447, -449, -468, and -469) at 350 and 450 μM Ni (as determined by colony size on streaked plates; data not shown). Either the nonpolar insertions in UR495 and UR497 failed to completely eliminate CooC activity in these strains, an unlikely possibility as the position and reading frame of the linker is different in each, or this variation reflects continued CooT and CooJ activities in the nonpolar mutants.

CooC

```
  1  MKIAVTGKGG VGKSTIVGML ARALSDEGWR VMAIDADPDA
 41  NLASAIGVPA ERLSALLPIS KMTGLARERT GASETTGTHF
 81  ILNPRVDDIP EQFCVDHAGI KLLLMGTVNH AGSGCVCPEH
121  ALVRTLLRHI LTKRKECVLI DMEAGIEHFG RGTIEAVDLL
161  VIVIEPGSRS LQTAAQIEGL ARDLGIKTIC HIANKLASPV
201  DVGFILDRAD QFDLLGSIPF DSAIQAADQA GLSCYDLSPA
241  CRDKAHALMA ALLERVGPTQ GVS*
```

CooT

```
  1  MCMAKVVLTK ADGGRVEIGD VLEVRAEGGA VRVTTLFDEE
 41  HAFPGLAIGR VDLRSGVISL IEEQNR*
```

CooJ

```
  1  MTESPERGRK RLGIYLAHFL DHVEGHMGEI GVQRDALAED
 41  ARLGALIDRA LADMAVARAS LNAVLRDLDG EAPAPASPEA
 81  VHSPFHSHAH SHDHDHAHGH SHDHAHDHCH CHDHP*
```

FIG. 2. Predicted products of *cooC*, *cooT*, and *cooJ*. The nucleotide-binding P-loop motif of CooC is overlined, and diamonds are placed above the histidine residues of CooJ. The line below the C terminus of CooJ indicates the region deleted in *R. rubrum* UR471.

Ni selectivity. The ability of UR479 (*cooT19*::*linker*) to grow better than wild-type *R. rubrum* in the absence of Ni addition led us to hypothesize that CooT is involved in metal discrimination. While its absence might then allow particularly efficient Ni incorporation, this model also implies that CO-dependent growth of the mutant could be more sensitive to metals known to readily bind apo-CODH in vitro. However, in medium supplemented with 0.5 μM Ni, CO-dependent growth of UR2, UR471, and UR479 was similarly inhibited by medium cobalt levels ≥300 μM, but unaffected by additions of 100 μM; 200 μM added Co reduced CO-dependent growth of all three strains (data not shown). We therefore have no evidence for a selectivity function dependent on the *cooTJ* gene products alone.

DISCUSSION

Microbial utilization of metals is affected by physical factors, including the metal species present, their concentrations and chelation by medium components (27), and the metabolic mechanisms that mediate metal transport, insure specific metal association with the apoprotein, and catalyze maturation to the holoenzyme (23).

In *R. rubrum* the products of *cooC* and *cooJ* are required for normal Ni processing into apo-CODH during CO-dependent growth, and mutations in *cooC*, *cooT*, or *cooJ* yield strains with distinctive Ni dependence phenotypes. It appears unlikely that *cooCTJ* products play a role in global Ni metabolism, Ni transport, or CODH processing for several reasons. In terms of global Ni metabolism, (i) Northern analysis indicates that transcription of *cooCTJ* is CO dependent (data not shown); (ii) mutation of these genes does not affect photoautotrophic growth; and (iii) CO-induced hydrogenase activity (CooH), a probable Ni enzyme, is little affected by the *cooC* polar insertion in strain UR294 (17). The products of *cooCTJ* are also unlikely to be involved in Ni transport because (i) their synthesis is not substantially different at 0 or 100 μM medium Ni concentration (determined by 2D-PAGE; data not shown); (ii) the proteins are not predicted to encode multiple transmembrane segments, in marked contrast to known Ni-transport components (42, 45); and (iii) the Ni requirement for CO-dependent growth is unaffected by a 10-fold decrease in medium Mg concentration (while higher levels of Ni became more toxic; data not shown; cf. reference 45). Finally, unlike most hydrogenase systems (17, 39), but analogous to urease systems (43, 44), there is no evidence for proteolytic processing of CooS: the enzyme from UR294 (*cooC7*::*kan*) is activated by Ni addition in vitro (17), as is the apoenzyme purified from wild-type cells grown in Ni-depleted medium (5, 13), and the enzyme's mobility on sodium dodecyl sulfate (SDS)-PAGE (5) and preparative native PAGE (13) is unaffected by the presence or absence of Ni.

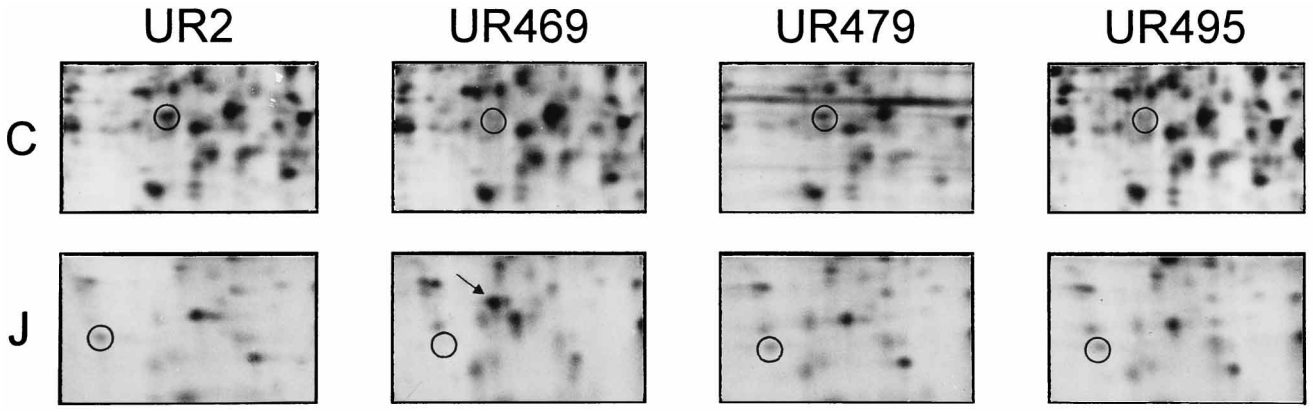

FIG. 3. 2D-PAGE of CooC and CooJ in CO-induced, [^{35}S]Met/Cys-pulse-labeled extracts from *R. rubrum* UR2 (wild type), UR469 (*cooC16*::*aacC1*Ω*linker*◂), UR479 (*cooT19*::*linker*), and UR495 (*cooC20*::*linker*). Two gel sections are presented, with the location of CooC indicated in the upper sections and the location of CooJ indicated in the lower sections. The second-dimension SDS-PAGE analysis used 15 and 17.5% acrylamide gels for analysis of CooC and CooJ, respectively. A spot noted in UR469 (arrow) is consistently associated with strains bearing the *aacC1*Ω*linker*◂ construct.

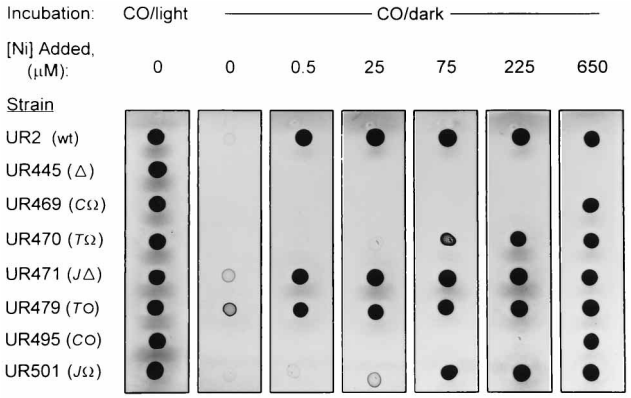

FIG. 4. Ni concentration dependence of photosynthetic and CO-dependent growth of *R. rubrum* strains. Cultures were spotted onto plates containing SAN medium supplemented with the indicated concentration of Ni and then incubated in the presence of CO either illuminated or in the dark. The medium contains acetate as a carbon source. Symbols adjacent to the strain numbers refer to the deletion of *cooFSCTJA* (△), the 60-bp internal deletion in *cooJ* (J△), or the presence of polar (Ω) or nonpolar (○) insertions.

Thus, we expect that the products of *cooC* and *cooJ* primarily catalyze Ni insertion into nascent CooS, though we cannot discount a role in Fe insertion. The in vitro activation experiments also suggest that some entity provides for metal selectivity, as apo-CODH itself binds Cd, Zn, Co, and Fe 2- to 300-fold more tightly than Ni, yielding essentially inactive enzyme (13). In an in vivo cobalt competition experiment we were unable to affiliate CooT or CooJ with metal specificity.

The most obvious similarities among the hydrogenase, urease, and CODH accessory systems are the nearly universal presence of nucleotide-binding and histidine-rich motifs. CooC, HypB, and UreG harbor a nucleotide binding-motif (Fig. 2) that is associated with low GTPase activity in certain HypB proteins (18, 40). The hydrogenase activity of *hypB E. coli* mutants requires exceptional Ni supplementation (0.5 mM; 29, 40, 59), while *Azotobacter* sp. *hypB* mutants require 10- to 50-fold less (8, 12). All *R. rubrum* strains bearing *cooC* mutations required Ni levels ca. 1,000-fold higher than that utilized to sustain wild-type CO-dependent growth (Fig. 4). That the polar and nonpolar *cooC* insertion mutants have similar Ni requirements indicates that the nonpolar insertions were sufficiently disruptive and that the phenotype is attributable to the loss of CooC alone, consistent with models wherein HypB and UreG proteins catalyze essential Ni insertion functions or conformational alterations of their respective apoprotein (39, 44).

The histidine-rich portion of CooJ is similar to motifs of HypB and UreE proteins, insofar as most contain several His residues, though their arrangement is inconstant (18, 50, 61) and is not evident in the *hyp* system of *E. coli* (39) or in the urease accessory systems of a *Bacillus* sp. (38) and *Helicobacter pylori* (10). Purified proteins bind three to nine Ni atoms per monomer and reportedly show either limited selectivity, typically binding Zn as well as Ni (18, 50), or a greater affinity for Ni at some of the binding sites (35). In CooJ (Fig. 2), as in *Rhodobacter capsulatus* HypB (61), the His residues are arrayed in a remarkably consistent alternating pattern.

The His-rich region of CooJ of *R. rubrum* was substantially dispensable, as the CO growth Ni dependence of strain UR471 (Δ*cooJ18*) matched that of the wild-type strain. Perhaps CooS activity is depressed but remains nonlimiting under these growth conditions, or perhaps the remaining C-terminal six-His component of the mutated CooJ retains sufficient function, a reasonable possibility given the aforementioned His-motif variations. Partial deletions in other systems are similarly leaky (38) (although conceivably an artifact of heterologous expression) and retain some ability to bind Ni in vitro (18). The His-rich region of the *Klebsiella aerogenes* UreE is likewise dispensable (6). The elevated Ni requirement of the *cooJ*::*aacC1*Ω*linker* strains UR500 and UR501 is analogous to results obtained with strains bearing more extensive *ureE* deletions: heterologous expression of *Proteus mirabilis* urease by a system lacking UreE required ca. 100-fold more Ni than did controls (55), and a deletion of *K. aerogenes ureE* (also expressed heterologously) produced a urease with depressed activity and lower Ni content (6, 34).

The reduced Ni dependence for CO growth of UR479 (*cooT19*::*linker*) is puzzling and heightens our interest in its function. The phenotypic difference between the *aacC1*Ω*linker* (UR451 and UR470) and *linker* (UR479) *cooT* insertion strains highlights the effect of polarity; in this case it is reasonable to assign the polar cassette insertion phenotype predominantly to lack of CooJ (as confirmed by 2D-PAGE) given the similar Ni dependence for CO growth of UR451/UR470 and UR500/UR501 (Fig. 4).

This analysis suggests both common and distinctive traits of the *cooCTJ* region compared to the accessory functions required for the urease and hydrogenase Ni metalloenzymes. The similarities probably reflect common Ni-processing functions, while the differences might be attributable to unique requirements and protein interactions. Given the prevalence of hydrogenase- and urease-associated accessory functions and the similarities between the Ni-CODHs analyzed to date, we expect that *cooCTJ* analogs will be found associated with all other Ni-CODH systems. Indeed, the *cooCTJ* functions may represent a minimum accessory complement if, for example, the *Clostridium thermoaceticum* CODH C center, site of CO oxidation, and A center, site of acetyl coenzyme A synthesis (33), require distinct Ni-insertion functions.

ACKNOWLEDGMENTS

This work was supported by The University of Wisconsin College of Agricultural and Life Sciences, Department of Energy grant DE-FG02-87ER13691, and National Institutes of Health grant GM53228.

We are grateful to Richard Watt, Nathan Spangler, and Doug Lies for discussions and use of unpublished data.

REFERENCES

1. **Allen, R. M., M. J. Homer, R. Chatterjee, P. W. Ludden, G. P. Roberts, and V. K. Shah.** 1993. Dinitrogenase reductase and MgATP-dependent maturation of apodinitrogenase from *Azotobacter vinelandii*. J. Biol. Chem. **268:** 23670–23674.
2. **Altschul, S. F., W. Gish, W. Miller, E. W. Myers, and D. J. Lipman.** 1990. Basic local alignment tool. J. Mol. Biol. **215:**403–410.
3. **Bonam, D., L. Lehman, G. P. Roberts, and P. W. Ludden.** 1989. Regulation of carbon monoxide dehydrogenase and hydrogenase in *Rhodospirillum rubrum*: effects of CO and oxygen on synthesis and activity. J. Bacteriol. **171:**3102–3107.
4. **Bonam, D., and P. W. Ludden.** 1987. Purification and characterization of carbon monoxide dehydrogenase, a nickel, zinc, iron-sulfur protein, from *Rhodospirillum rubrum*. J. Biol. Chem. **262:**2980–2987.
5. **Bonam, D., M. C. McKenna, P. J. Stephens, and P. W. Ludden.** 1988. Nickel-deficient carbon monoxide dehydrogenase from *Rhodospirillum rubrum*: *in vivo* and *in vitro* activation by exogenous nickel. Proc. Natl. Acad. Sci. USA **85:**31–35.
6. **Brayman, T. G., and R. P. Hausinger.** 1996. Purification, characterization, and functional analysis of a truncated *Klebsiella aerogenes* UreE urease accessory protein lacking the histidine-rich carboxyl terminus. J. Bacteriol. **178:**5410–5416.
7. **Bult, C. J., et al.** 1996. Complete genome sequence of the methanogenic archaeon, *Methanococcus jannaschii*. Science **273:**1058–1073.
8. **Chen, J. C., L. E. Mortenson, and L. C. Seefeldt.** 1995. Analysis of a gene region required for dihydrogen oxidation in *Azotobacter vinelandii*. Curr. Microbiol. **30:**351–355.

9. **Coppoc, L. J.** 1991. M.S. thesis. University of Wisconsin, Madison.
10. **Cussac, V., R. L. Ferrero, and A. Labigne.** 1992. Expression of *Helicobacter pylori* urease genes in *Escherichia coli* grown under nitrogen-limiting conditions. J. Bacteriol. **174:**2466–2473.
11. **Dernedde, J., T. Eitinger, N. Patenge, and B. Friedrich.** 1996. *hyp* gene products in *Alcaligenes eutrophus* are part of a hydrogenase-maturation system. Eur. J. Biochem. **235:**351–358.
12. **Du, L., and K. H. Tibelius.** 1994. The *hupB* gene of the *Azotobacter chroococcum* hydrogenase gene cluster is involved in nickel metabolism. Curr. Microbiol. **28:**21–24.
13. **Ensign, S. A., M. J. Campbell, and P. W. Ludden.** 1990. Activation of the nickel-deficient carbon monoxide dehydrogenase from *Rhodospirillum rubrum*: kinetic characterization and reductant requirement. Biochemistry **29:** 2162–2168.
14. **Ensign, S. A., and P. W. Ludden.** 1991. Characterization of the CO oxidation/H_2 evolution system of *Rhodospirillum rubrum*: role of a 22-kDa iron-sulfur protein in mediating electron transfer between carbon monoxide dehydrogenase and hydrogenase. J. Biol. Chem. **266:**18395–18403.
15. **Ferry, J. G.** 1995. CO dehydrogenase. Annu. Rev. Microbiol. **49:**305–333.
16. **Fox, J. D., Y. He, D. Shelver, G. P. Roberts, and P. W. Ludden.** 1996. Characterization of the region encoding the CO-induced hydrogenase of *Rhodospirillum rubrum*. J. Bacteriol. **178:**6200–6208.
17. **Fox, J. D., R. L. Kerby, G. P. Roberts, and P. W. Ludden.** 1996. Characterization of the CO-induced, CO-tolerant hydrogenase from *Rhodospirillum rubrum* and the gene encoding the large subunit of the enzyme. J. Bacteriol. **178:**1515–1524.
18. **Fu, C., J. W. Olson, and R. J. Maier.** 1995. HypB protein of *Bradyrhizobium japonicum* is a metal-binding GTPase capable of binding 18 divalent nickel ions per dimer. Proc. Natl. Acad. Sci. USA **92:**2333–2337.
19. **Genetics Computer Group.** 1994. Program manual for the Wisconsin package, version 8. Genetics Computer Group, Madison, Wis.
20. **Gilbert, J. V., J. Ramakrishna, F. W. Sunderman, Jr., A. Wright, and A. G. Plaut.** 1995. Protein Hpn: cloning and characterization of a histidine-rich metal-binding polypeptide in *Helicobacter pylori* and *Helicobacter mustelae*. Infect. Immun. **63:**2682–2688.
21. **Goff, S. P., and V. R. Prasad.** 1991. Linker insertion mutagenesis as probe of structure-function relationships. Methods Enzymol. **208:**586–603.
22. **Grunwald, S. K., D. P. Lies, G. P. Roberts, and P. W. Ludden.** 1995. Posttranslational regulation of nitrogenase in *Rhodospirillum rubrum* strains overexpressing the regulatory enzymes dinitrogenase reductase ADP-ribosyltransferase and dinitrogenase reductase activating glycohydrolase. J. Bacteriol. **177:**628–635.
23. **Hausinger, R. P.** 1996. General principles and mechanisms of metallocenter assembly, p. 1–18. *In* R. P. Hausinger, G. L. Eichhorn, and L. G. Marzilli, (ed.), Mechanisms of metallocenter assembly. VCH Publishers, Inc., New York, N.Y.
24. **He, Y., D. Shelver, R. L. Kerby, and G. P. Roberts.** 1996. Characterization of a CO-responsive transcriptional activator from *Rhodospirillum rubrum*. J. Biol. Chem. **271:**120–123.
25. **Hong, S. S., and G. P. Roberts.** Unpublished data.
26. **Hu, Z., N. J. Spangler, M. E. Anderson, J. Xia, P. W. Ludden, P. A. Lindahl, and E. Münck.** 1996. Nature of the C-cluster in Ni-containing carbon monoxide dehydrogenases. J. Am. Chem. Soc. **118:**830–845.
27. **Hughes, M. N., and R. K. Poole.** 1991. Metal speciation and microbial growth—the hard (and soft) facts. J. Gen. Microbiol. **137:**725–734.
28. **Island, M. D., and H. L. T. Mobley.** 1995. *Proteus mirabilis* urease: operon fusion and linker insertion analysis of *ure* gene organization, regulation, and function. J. Bacteriol. **177:**5653–5660.
29. **Jacobi, A., R. Rossmann, and A. Böck.** 1992. The *hyp* operon gene products are required for the maturation of catalytically active hydrogenase isoenzymes in *Escherichia coli*. Arch. Microbiol. **158:**444–451.
30. **Kerby, R. L., S. S. Hong, S. A. Ensign, L. J. Coppoc, P. W. Ludden, and G. P. Roberts.** 1992. Genetic and physiological characterization of the *Rhodospirillum rubrum* carbon monoxide dehydrogenase system. J. Bacteriol. **174:** 5284–5294.
31. **Kerby, R. L., P. W. Ludden, and G. P. Roberts.** 1995. Carbon monoxide-dependent growth of *Rhodospirillum rubrum*. J. Bacteriol. **177:**2241–2244.
32. **Kolodziej, P. A., and R. A. Young.** 1991. Epitope tagging and protein surveillance. Methods Enzymol. **194:**508–519.
33. **Kumar, M., D. Qiu, T. G. Spiro, and S. W. Ragsdale.** 1995. A methylnickel intermediate in a bimetallic mechanism of acetyl-coenzyme A synthesis by anaerobic bacteria. Science **270:**628–630.
34. **Lee, M. H., S. B. Mulrooney, M. J. Renner, Y. Markowicz, and R. P. Hausinger.** 1992. *Klebsiella aerogenes* urease gene cluster: sequence of *ureD* and demonstration that four accessory genes (*ureD*, *ureE*, *ureF*, and *ureG*) are involved in nickel metallocenter biosynthesis. J. Bacteriol. **174:**4324–4330.
35. **Lee, M. H., H. S. Pankratz, S. Wang, R. A. Scott, M. G. Finnegan, M. K. Johnson, J. A. Ippolito, D. W. Christianson, and R. P. Hausinger.** 1993. Purification and characterization of *Klebsiella aerogenes* UreE protein: a nickel-binding protein that functions in urease metallocenter assembly. Protein Sci. **2:**1042–1052.
36. **Lies, D. L., and G. P. Roberts.** Unpublished data.
37. **Ludden, P. W., and G. P. Roberts.** 1995. The biochemistry and genetics of nitrogen fixation by photosynthetic bacteria, p. 929–947. *In* R. E. Blankenship, M. T. Madigan, and C. E. Bauer (ed.), Anoxygenic photosynthetic bacteria. Kluwer Academic Publishers, Dordrecht, The Netherlands.
38. **Maeda, M., M. Hidaka, A. Nakamura, H. Masaki, and T. Uozumi.** 1994. Cloning, sequencing, and expression of thermophilic *Bacillus* sp. strain TB-90 urease gene complex in *Escherichia coli*. J. Bacteriol. **176:**432–442.
39. **Maier, T., and A. Böck.** 1996. Nickel incorporation into hydrogenases, p. 173–192. *In* R. P. Hausinger, G. L. Eichhorn, and L. G. Marzilli, (ed.), Mechanisms of metallocenter assembly. VCH Publishers, Inc., New York, N.Y.
40. **Maier, T., F. Lottspeich, and A. Böck.** 1995. GTP hydrolysis by HypB is essential for nickel insertion into hydrogenases of *Escherichia coli*. Eur. J. Biochem. **230:**133–138.
41. **Maupin-Furlow, J. A., and J. G. Ferry.** 1996. Analysis of the CO dehydrogenase/acetyl-coenzyme A synthase operon of *Methanosarcina thermophila*. J. Bacteriol. **178:**6849–6856.
42. **Mobley, H. L. T., R. M. Garner, and P. Bauerfeind.** 1995. *Helicobacter pylori* nickel-transport gene *nixA*: synthesis of catalytically active urease in *Escherichia coli* independent of growth conditions. Mol. Microbiol. **16:**97–109.
43. **Mobley, H. L. T., M. D. Island, and R. P. Hausinger.** 1995. Molecular biology of microbial ureases. Microbiol. Rev. **59:**451–480.
44. **Moncrief, M. B. C., and R. P. Hausinger.** 1996. Nickel incorporation into urease, p. 151–171. *In* R. P. Hausinger, G. L. Eichhorn, and L. G. Marzilli, (ed.), Mechanisms of metallocenter assembly. VCH Publishers, Inc., New York, N.Y.
45. **Navarro, C., L.-F. Wu, and M.-A. Mandrand-Berthelot.** 1993. The *nik* operon of *Escherichia coli* encodes a periplasmic binding-protein-dependent transport system for nickel. Mol. Microbiol. **9:**1181–1191.
46. **Oliphant, A. R., and K. Struhl.** 1987. The use of random-sequence oligonucleotides for determining consensus sequences. Methods Enzymol. **155:**568–582.
47. **Parker, R. C., R. M. Watson, and J. Vinograd.** 1977. Mapping of closed circular DNAs by cleavage with restriction endonucleases and calibration by agarose gel electrophoresis. Proc. Natl. Acad. Sci. USA **74:**851–855.
48. **Peters, J. W., K. Fisher, and D. R. Dean.** 1995. Nitrogenase structure and function: a biochemical-genetic perspective. Annu. Rev. Microbiol. **49:**335–366.
49. **Prentki, P., and H. M. Krisch.** 1984. In vitro insertional mutagenesis with a selectable DNA fragment. Gene **29:**303–313.
50. **Rey, L., J. Imperial, J.-M. Palacios, and T. Ruiz-Argüeso.** 1994. Purification of *Rhizobium leguminosarum* HypB, a nickel-binding protein required for hydrogenase synthesis. J. Bacteriol. **176:**6066–6073.
51. **Sambrook, J., E. F. Fritsch, and T. Maniatis.** 1989. Molecular cloning: a laboratory manual, 2nd ed. Cold Spring Harbor Laboratory, Cold Spring Harbor, N.Y.
52. **Schweizer, H. P.** 1993. Small broad-host-range gentamycin resistance gene cassettes for site-specific insertion and deletion mutagenesis. BioTechniques **15:**831–834.
53. **Shelver, D., R. L. Kerby, Y. He, and G. P. Roberts.** 1995. Carbon monoxide-induced activation of gene expression in *Rhodospirillum rubrum* requires the product of *cooA*, a member of the cyclic AMP receptor protein family of transcriptional regulators. J. Bacteriol. **177:**2157–2163.
54. **Simon, R., U. Priefer, and A. Pühler.** 1983. A broad host range mobilization system for *in vivo* genetic engineering: transposon mutagenesis in gram negative bacteria. Bio/Technology **1:**784–791.
55. **Sriwanthana, B., M. D. Island, D. Maneval, and H. L. T. Mobley.** 1994. Single-step purification of *Proteus mirabilis* urease accessory protein UreE, a protein with a naturally occurring histidine tail, by nickel chelate affinity chromatography. J. Bacteriol. **176:**6836–6841.
56. **Stultz, C. M., J. V. White, and T. F. Smith.** 1993. Structural analysis based on state-space modeling. Protein Sci. **2:**305–314.
57. **Thauer, R. K., and L. G. Bonacker.** 1994. Biosynthesis of coenzyme F_{430}, a nickel porphinoid involved in methanogenesis. CIBA Found. Symp. **180:**210–227.
58. **Watt, R. K., and P. W. Ludden.** Unpublished data.
59. **Waugh, R., and D. H. Boxer.** 1986. Pleiotropic hydrogenase mutants of *Escherichia coli* K12: growth in the presence of nickel can restore hydrogenase activity. Biochimie **68:**157–166.
60. **White, J. V., C. M. Stultz, and T. F. Smith.** 1994. Protein classification by stochastic modeling and optimal filtering of amino-acid sequences. Math. Biosci. **119:**35–75.
61. **Xu, H.-W., and J. D. Wall.** 1991. Clustering of genes necessary for hydrogen oxidation in *Rhodobacter capsulatus*. J. Bacteriol. **173:**2401–2405.